Journal of Materials Chemistry C

Accepted Manuscript

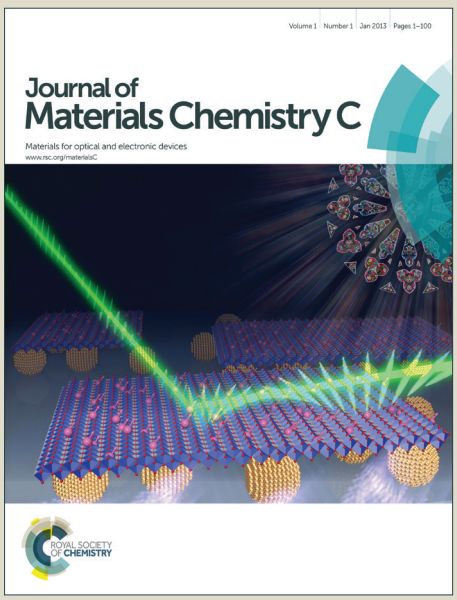

ROYAL SOCIETY OF CHEMISTRY

www.rsc.org/materialsC

Journal Name

RSCPublishing

ARTICLE

Multi-color Luminescence of Uniform $CdWO_4$ Nanorods through Eu^{3+} Ion Doping

Cite this: DOI: 10.1039/xoxxoooooox

Dan Yue,[a,b] Qingfeng Li,[a] Wei Lu,[c] Qi Wang,[a] Mengnan Wang,[a,b] Chunyang Li,[a] Lin Jin,[a] Yurong Shi,[a] Zhenling Wang,[*,a] Jianhua Hao[*,d]

Received ooth January 2012,
Accepted ooth January 2012

DOI: 10.1039/xoxxoooooox

www.rsc.org/

Uniform Eu^{3+} doped $CdWO_4$ nanorods were prepared via a simple hydrothermal method and characterized by X-ray diffraction, transmission electron microscopy, photoluminescence (PL) spectroscopy and PL lifetime measurement. The results indicate that the obtained Eu^{3+} doped $CdWO_4$ nanorods have monoclinic phase structure, and the phase structure can be retained at Eu^{3+} doping concentrations of 0.4%~4.0%. The diameter of nanorods decreases from 27 to 15 nm with an increase in the doping concentrations, and the morphology becomes irregular at the Eu^{3+} doping concentration of 6.5%. Under the excitation of ultraviolet light, the relative intensities of blue-green emission ascribed to WO_4^{2-} and red emission from Eu^{3+} can be tuned through doping Eu^{3+} ions into the $CdWO_4$ nanorods and thus altering the energy transfer between WO_4^{2-} and Eu^{3+}. Hence, the multi-color luminescence in a same host under single excited wavelength can be realized simply by altering the doping concentration of Eu^{3+}. These luminescent nanomaterials may have potential applications in displays, light sources, bio-imaging and so on.

Introduction

Metal tungstates have been widely investigated because of their potential applications in various fields, such as sensors, photonics, magnetic devices, photocatalysis, etc.[1-8] As one typical example among them, $CdWO_4$ has been considered to be a conventional functional material due to its high average refractive index, low radiation damage and excellent X-ray absorption coefficient.[9] To date, most efforts for the preparation of $CdWO_4$ have mainly been devoted to the forms of single crystals, powders and films, and accordingly the functional properties such as photocatalytic activity have been studied systematically.[10-12] For example, monoclinic and tetragonal structured $CdWO_4$ nanocrystals can be effectively synthesized by hydrothermal method, and the monoclinic $CdWO_4$ nanocrystal exhibited a much higher photocatalytic performance than the tetragonal one for degrading methyl orange under ultraviolet (UV) light illumination.[13] Furthermore, reduced graphene oxide (RGO) hybridized $CdWO_4$ shows much higher photocatalytic activity than pure $CdWO_4$ for methylene blue degradation, because the RGO can attract the photo-generated electrons and thus help to reduce the recombination rate of photo-generated charges.[14] Ye et al found that Eu^{3+}-doped $CdWO_4$ could enhance photocatalytic activity in the photodegradation of methyl orange.[15] Recently, Eu^{3+}-doped $CdWO_4$ nanocrystals have been synthesized as red phosphor for white-LED,[16] and Dai et al have investigated the surface defects and their influence on the structural and PL properties of $CdWO_4$:Eu^{3+} nanocrystals.[17] However, there are few papers reported on the synthesis of uniform rare-earth ion (RE^{3+}) doped $CdWO_4$ nanorods, and the energy transfer between $CdWO_4$ host and the doping RE^{3+} has not investigated systematically. Moreover, the multi-color luminescence in $CdWO_4$ host through doping RE^{3+} has not yet been reported. The intrinsic emission of $CaWO_4$ phosphor has been confirmed to present a broad emission band centred at ~420 nm due to electronic transitions of the charge-transfer type between oxygen and W^{6+} within the anion complex WO_4^{2-}, and $CaWO_4$:Tb^{3+} particles exhibit bright green emission arising from the efficient energy transfer from WO_4^{2-} groups to Tb^{3+} ions.[18] Similarly, RE^{3+} doped $CdWO_4$ nanorods could exhibit a broad emission band of WO_4^{2-} groups and line emissions corresponding to f-f transitions of RE^{3+}, and the efficient energy transfer from WO_4^{2-} groups in $CdWO_4$ nanorods to doping RE^{3+} ions might be occurred as well.[19,20] The luminescent properties, such as multi-color luminescence and emission intensity of $CdWO_4$:RE^{3+} nanorods could possibly be controlled through altering the doping concentration and kinds of RE^{3+} ion, and affecting the efficiency of energy transfer from WO_4^{2-} groups to RE^{3+}.

In this work, Eu^{3+} doped $CdWO_4$ nanorods were successfully synthesized through a simple hydrothermal method and characterized by X-ray diffraction (XRD), transmission electron microscopy (TEM), PL and lifetime techniques. The obtained $CdWO_4$:Eu^{3+} nanorods are uniform and the diameter of these nanorods can be controlled by altering the doping concentrations of Eu^{3+} ions. Furthermore, the luminescent color of $CdWO_4$ nanorods

can be tuned from blue-green to white and red emissions through altering the doping concentrations of Eu^{3+}. The multi-color luminescence of the same host under single excited wavelength can be realized by simply changing the doping concentrations of Eu^{3+}. These $CdWO_4$:Eu^{3+} nanorods with uniform size and prominent luminescence properties show promise for various applications in the fields of displays, bio-imaging and white-LEDs.

Experimental

Synthesis

All chemicals were used directly without further purification. $Cd(NO_3)_2\,4H_2O$ (99.99%, analytical grade reagents, A. R.) and $Na_2WO_4\,2H_2O$ (≥99.0%, A. R.) were obtained from Sinopharm Chemical Reagent Co., Ltd. $Eu(NO_3)_3$ solution was prepared by dissolving Eu_2O_3 (99.99%) in diluted nitric acid. $CdWO_4$ nanorods were prepared by hydrothermal technique. Typically, 10.0 mL of 0.25 mol/L Na_2WO_4 was added to 10.0 mL of 0.25 mol/L $Cd(NO_3)_2$ aqueous solution and the mixture was continuously stirred for 0.5 h. The obtained suspension was then transferred into a Teflon bottle held in a stainless steel autoclave, which was sealed and hydrothermally treated at 160 ^oC for 22 h. After the autoclave was cooled to room temperature naturally, the precipitates were separated by centrifugation, washed with ethanol and distilled water twice respectively, and dried at 50 ^oC for 24 h to obtain the sample. Additionally, $CdWO_4$:x%Eu^{3+} samples with different dopant concentrations (x = 0.4, 1.2, 2.0, 4.0, 6.5) were selected in order to investigate the effects of doping concentrations on the luminescent properties, morphology and phase structure. The synthesis procedure was similar to that mentioned above except that 10.0 mL of 0.25 mol/L Na_2WO_4 was added to the mixed solutions of $Cd(NO_3)_2$ and $Eu(NO_3)_3$ with a desired molar ratio, and the other conditions were identical.

Characterization

Phase structure was characterized by a Bruker D8 Advance X-ray diffractometer (XRD) with Cu-Kα radiation (λ = 0.15406 nm). The accelerating voltage and emission current were 40 kV and 40 mA, respectively. The TEM image, selected area electron diffraction (SAED) pattern and energy dispersive X-ray spectrum (EDS) were obtained on a JEOL-2010 transmission electron microscope and JEOL-2100F scanning transmission electron microscope (STEM) equipped with an Oxford INCA x-sight EDS Si (Li) detector at an accelerating voltage of 200 kV. PL spectra and lifetime test were carried out using an FLS920P Edinburgh Analytical Instrument apparatus equipped with a 450 W Xenon lamp and a μF900H high-energy microsecond flash lamp as the excitation sources. Quantum yields of the samples were measured using a $BaSO_4$-coated integrating sphere of diameter 15 cm in FLS920 based on the absolute method. Excitation 290 nm and emission at 475 or 615 nm were selected. The slit widths for the excitation and emission tests were fixed at 5.0 and 0.2 nm, respectively. The step size was 0.2 nm and the integration time was 0.3 s. All of the measurements were performed at room temperature.

Results and discussion

The phase structure of undoped and Eu^{3+} doped $CdWO_4$ nanorods were analyzed by XRD technique. Fig. 1a shows the XRD patterns of $CdWO_4$: Eu^{3+} nanorods with the doping concentrations of 0%, 0.4%, 1.2%, 2.0%, 4.0% and 6.5%. When the doping concentration of Eu^{3+} was less than 6.5%, all the diffraction peaks in the patterns matched well with the standard data for the monoclinic structure of bulk $CdWO_4$ (JCPDS No. 14-0676) with the space groups of P2/c. No peaks corresponding to any other phases or impurities were detected, suggesting the high purity of these samples within the doping concentration range from 0.4% to 4.0%. In this phase structure, each W is surrounded by four nearest oxygen ions and two more distant ones in approximately octahedral coordination to form a WO_6^{6-} molecular complex.[13] However, when increasing the Eu^{3+} doping concentration to 6.5%, several weak diffraction peaks marked as star were present, which is identified to the monoclinic phase of Eu_2O_3 (JCPDS No. 34-0072). Fig. 1b shows the (-111) and (111) diffraction peaks of $CdWO_4$:x%Eu^{3+} in the measured range of $2\theta = 28^o\sim31^o$, and the diffraction peaks of $CdWO_4$ are shifted slightly to the higher angle with an increase in Eu^{3+} doping concentration. The ionic radii of Cd^{2+} with 6 CN (CN = coordination number) in monoclinic phase is 0.95 Å, which is slightly larger than that of the corresponding Eu^{3+} ion (0.947 Å).[21,22] Hence, it is reasonable to observe the peak shift towards higher 2θ, and to some extent the results might imply that Eu^{3+} is homogeneously incorporated into the lattice of $CdWO_4$ and occupied the sites of Cd^{2+}. Due to the close ionic radii of Cd^{2+} and Eu^{3+} ions, the values of the calculated lattice parameters and unit cell volume of Eu^{3+} doped $CdWO_4$ nanorods are very similar to those of the undoped sample, as listed in Table 1. When Eu^{3+} ions are doped into the $CdWO_4$ host lattice, they would chemically non-equivalently substitute the Cd^{2+} sites, thus an excess of positive charge in the lattice must be compensated. One possible way is that two Eu^{3+} ions replace three Cd^{2+} ions to balance the charge of this compound, which creates two Eu_{Cd}° positive defects and one $V_{Cd}^{''}$ negative defect as follows:[20,23]

$$2Eu^{3+} + 3Cd^{2+} \rightarrow 2Eu_{Cd}^{\circ} + V_{Cd}^{''} \quad (1)$$

The oxygen adjacent to the Cd^{2+} might slightly deviate the original lattice site, which probably leads to the distortion of the WO_6^{6-} molecular complex in order to accommodate the positive and negative defects.

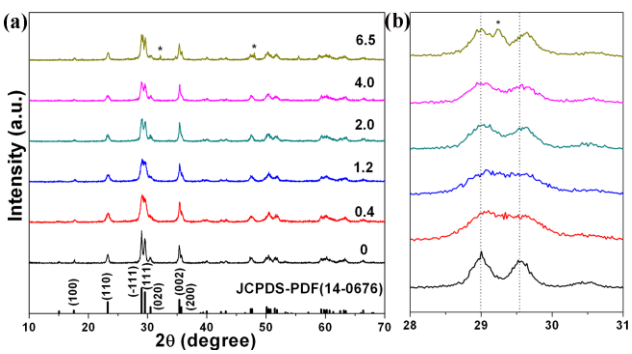

Fig. 1 (a) XRD patterns of $CdWO_4$:x%Eu^{3+} with different concentrations (x = 0, 0.4, 1.2, 2.0, 4.0, 6.5) and the standard data for bulk $CdWO_4$ (JCPDS card No. 14-0676); (b) Diffraction peak positions of $CdWO_4$:x%Eu^{3+} in the range of $2\theta = 28^o$ to 31^o (The secondary phase marked by "*").

Table 1 Lattice parameters and unit cell volume of $CdWO_4$:x%Eu^{3+} with different concentrations (x = 0, 0.4, 1.2, 2.0, 4.0, 6.5)

Samples	Lattice parameters			
	a (nm)	**b (nm)**	**c (nm)**	**unit cell volume($Å^3$)**
$CdWO_4$	0.5017	0.5852	0.5067	148.77
$CdWO_4$:0.4%Eu^{3+}	0.5038	0.5836	0.5074	149.14
$CdWO_4$:1.2%Eu^{3+}	0.5035	0.5849	0.5071	149.31
$CdWO_4$:2.0%Eu^{3+}	0.5046	0.5859	0.5079	150.11
$CdWO_4$:4.0%Eu^{3+}	0.5022	0.5845	0.5060	148.47
$CdWO_4$:6.5%Eu^{3+}	0.5018	0.5852	0.5073	148.92

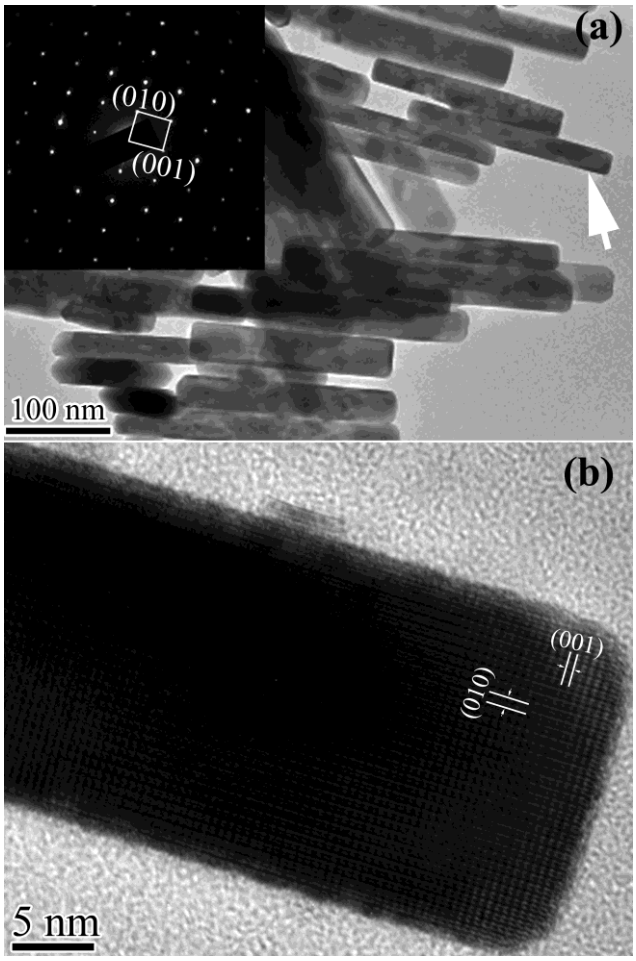

Fig. 2 (a) TEM and (b) HRTEM images of $CdWO_4$ nanorods (Inset is the SAED of the single nanorod).

Fig. 2 shows typical TEM images of undoped $CdWO_4$ nanorods. It can be clearly seen from Fig. 2a that the obtained sample is composed of uniform nanorods with the diameter of ~27 nm and the length of ~200 nm. The SAED pattern (Fig. 2a, inset) taken from the upper single nanorod can be indexed to the (010) and (001) planes of $CdWO_4$ single crystalline with the monoclinic phase structure. These findings are consistent with the XRD result as above illustrated. The HRTEM image (Fig. 2b) of the single $CdWO_4$ nanorod marked as an arrow in Fig. 2a displays single crystalline nature. The values of interplanar spacing of $CdWO_4$ nanorod are 0.586 and 0.507 nm, which is identical to the (010) and (001) facet distance of bulk $CdWO_4$ powders, respectively. The growth direction of $CdWO_4$ single crystalline nanorod is along the direction perpendicular to (001) plane.

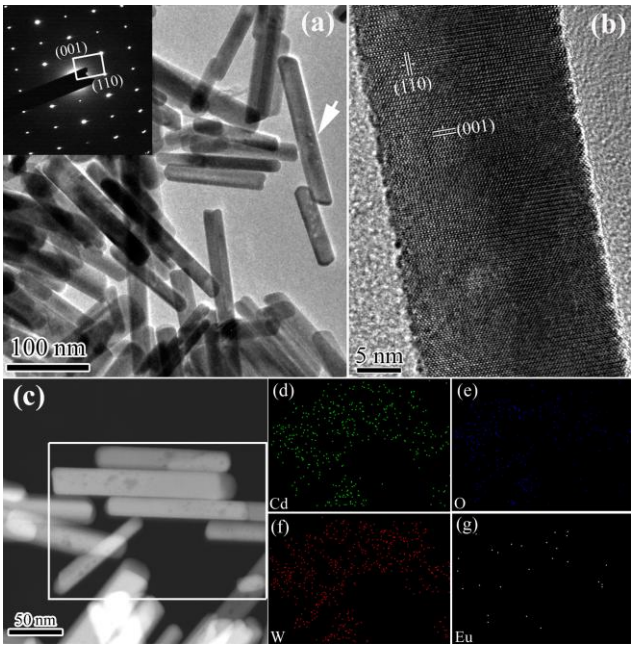

Fig. 3 (a) TEM and (b) HRTEM images of $CdWO_4$:2.0%Eu^{3+} nanorods (Inset is the SAED of the single nanorod); (c) STEM-HAADF image of $CdWO_4$:2.0%Eu^{3+} nanorods, and (d~g) EDS element mappings for Cd, O, W and Eu of the nanorods shown in (c) respectively.

The morphology of $CdWO_4$ nanorods is not changed prominently when the doping concentration of Eu^{3+} is at a relatively low concentration range of 0.4% ~ 4%. Fig. 3 shows typical TEM images and EDS element mappings of $CdWO_4$:2.0%Eu^{3+} nanorods. It can be seen that the morphology of $CdWO_4$:2.0%Eu^{3+} is similar to that of the undoped sample, composed of nanorods with the diameter of ~25 nm and the length of ~150 nm. The SAED pattern (Fig. 3a, inset) taken from a single nanorod can be indexed to the (110) and (001) planes of $CdWO_4$ single crystalline with the monoclinic phase structure. From the HRTEM image of a single $CdWO_4$:2.0%Eu^{3+} nanorod, it can be measured that the interplanar spacing is about 0.507 nm and 0.382 nm, corresponding to the (001) and (110) planes of $CdWO_4$, respectively, and the growth direction of the single crystalline $CdWO_4$:2.0%Eu^{3+} nanorod is along the direction perpendicular to (001) plane as well. Fig. 3c shows the morphology of $CdWO_4$:2.0%Eu^{3+} nanorods acquired in STEM-HAADF (high angle annular dark field) topology mode. The EDS element

mappings of Cd (Fig. 3d), O (Fig. 3e), W (Fig. 3f) and Eu (Fig. 3g) elements show that the nanorods are composed of Cd, O and W elements with doped Eu randomly. It indicates that the Eu^{3+} doping at relatively low concentrations has little effect on the phase structure, single crystalline feature and the growth direction of $CdWO_4$ nanorods. However, the values of the width and length of $CdWO_4$ nanorods showed a decrease trend when increasing Eu^{3+} doping concentrations, and the morphology of $CdWO_4$ nanorods became irregular when the Eu^{3+} doping concentration was increased up to 6.5%, as shown in Fig. S1 (ESI†). The reason that the size of nanorods gradually decreases with an increase in doping concentration may be partly attributed to the strong effect of the dopant ion on the crystal growth rate through surface charge modification.[24] This size evolution trend of nanorods is consistent with previous reports on the Gd^{3+} or Eu^{3+} doped $NaYF_4$ and Ce^{3+} doped $LaPO_4$ nanorods.[24-26]

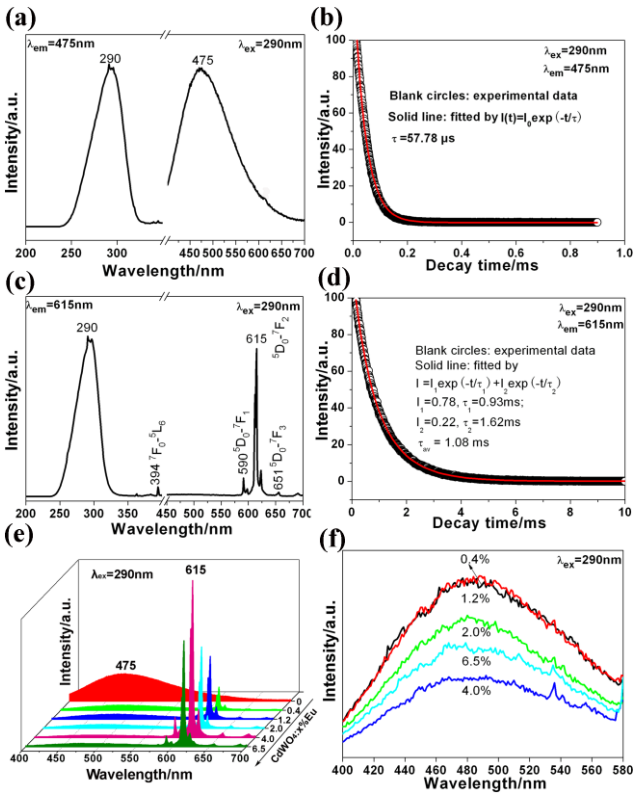

Fig. 4 (a) PL excitation and emission spectra and (b) luminescent decay curve of $CdWO_4$ nanorods, (c) PL excitation and emission spectra and (d) luminescent decay curve of $CdWO_4$:4.0%Eu^{3+} nanorods, and (e, f) PL emission spectra of $CdWO_4$:x%Eu^{3+} samples with different doping concentrations.

The luminescent properties of the undoped and Eu^{3+} doped $CdWO_4$ samples were investigated by PL spectra and decay curves. In Fig. 4a (left), an intense excitation band from 230 to 350 nm with a maximum at 290 nm is observed, which is attributed to the charge transfer transition from the oxygen (O) 2p orbits to one of the empty tungsten (W) 5d orbits within the WO_4^{2-} groups.[27,28] Excited by 290 nm UV light, $CdWO_4$ nanorods exhibit a blue-green emission band in the range of 400~700 nm with the emission peak centred at 475 nm, as shown in Fig. 4a (right). The PL decay curve of $CdWO_4$ nanorods (Fig. 4b) can be well fitted into a single exponential function as

$$I(t) = I_0 \exp(-t/\tau) \quad (2)$$

where I_0 is the initial intensity at $t = 0$, τ is the 1/e lifetime of the lanthanide ions. The lifetime (τ) of $CdWO_4$ nanorods is determined to be 57.78 μs.

Fig. 4c (left) shows the excitation spectrum of $CdWO_4$:4.0%Eu^{3+} nanorods. Similarly, the excitation spectrum monitored at 615 nm shows a broad excitation band at the range of 230~350 nm with the peak at 290 nm, which is assigned to the O→W ligand-to-metal charge transfer from WO_4^{2-} groups.[29,30] Meanwhile, the excitation peak at around 394 nm is assigned to the $^7F_0 \rightarrow {}^5L_6$ transitions of Eu^{3+} ions. The emission spectrum (Fig. 4c, right) is mainly composed of $^5D_0 \rightarrow {}^7F_J$ (J = 1, 2, 3) emission lines of Eu^{3+} ions from 550 to 700 nm. Compared with the emission peaks of Eu^{3+}, the intrinsic blue-green emission from WO_4^{2-} groups is very weak, suggesting the existence of an efficient energy transfer from WO_4^{2-} groups to the doping Eu^{3+}. It is known that the relative intensities of the $^5D_0 \rightarrow {}^7F_1$ and $^5D_0 \rightarrow {}^7F_2$ emissions are very sensitive to the detailed nature of ligand environment.[31,32] On a site without inversion symmetry, the $^5D_0 \rightarrow {}^7F_2$ electric dipole transition is strongest. The electric dipole transition is allowed only under the condition that the Eu^{3+} ion occupies a site without an inversion centre.[33] In the $CdWO_4$:4.0%Eu^{3+} nanorods, the Eu^{3+} ions occupy the Cd^{2+} ions lattice at a site without inversion symmetry in $CdWO_4$ matrix, therefore the dominated emission centred at 615 nm corresponds to $^5D_0 \rightarrow {}^7F_2$ electric dipole transition.[34]

The luminescent decay curve of $CdWO_4$:4.0%Eu^{3+} nanorods (Fig. 4d) can be well fitted into the following double exponential function instead of a single exponential function.

$$I = I_1 \exp(-t/\tau_1) + I_2 \exp(-t/\tau_2) \quad (3)$$

where I_1 and I_2 are the intensities at different time interval, while τ_1 and τ_2 are their corresponding lifetimes. For solid-state luminescent materials in which there exists energy transfer process, when the host materials or sensitizers are excited (indirect excitation), some luminescence decay curves from the rare-earth activator could follow non-exponential function (eq. 4) in the case of $GdPO_4$: Tb^{3+}/Ce^{3+}, $CaMoO_4$: Tb^{3+}, $LaVO_4$: Eu^{3+}, etc.,

$$I = I_0 e^{(-t/\tau - Dt^{0.5})} \quad (4)$$

where D is related to diffusion and energy transfer.[22,35] At the same time, there are other luminescence decay curves that obey double exponential function in many luminescence materials, such as rare earth tungstate and molybdate compounds, lanthanide-doped upconversion nanoparticles, and so on.[36] It should be denoted that the luminescence decay behavior might simultaneously follow the double exponential function and non-exponential function even for the same luminescent materials (like $CaMoO_4$: Tb^{3+} nanoparticles), except for the slight difference of the parameter goodness.[35a] As for $CdWO_4$:x%Eu^{3+} nanorods, there exists an energy transfer from

WO_4^{2-} to Eu^{3+} excitation at 290 nm, and this is followed by the luminescence decay from $^5D_0$ level of Eu^{3+}. It can be seen from Fig. S2 (ESI†) that all luminescent decay curves of $CdWO_4$:x%Eu^{3+} (x = 0.4, 1.2, 2.0, 4.0, 6.5) can be well fitted into the double exponential function, and the goodness of parameter is found to be 0.9997, 0.9993, 0.9995, 0.9995 and 0.9995, respectively. These values of the parameter goodness are well enough and the double exponential fitting is satisfying, although the luminescent decay curves of $CdWO_4$:x%Eu^{3+} might follow the non-exponential behavior as well. Parchur *et al.*[35a,37] reported that if the particles are spherical, the sphere can be divided into two shells of equal volume. Inner shell ions have a longer lifetime than outer shell ions. Based on this, the average lifetime τ_{av} can be calculated using the following equation:

$$\tau_{av} = (I_1\tau_1^2 + I_2\tau_2^2)/(I_1\tau_1 + I_2\tau_2) \quad (5)$$

However, for the luminescent materials with non-spherical morphology such as $CdWO_4$:Eu^{3+} nanorods in this work, the average lifetime τ_{av} can be determined by the formula as [38]

$$\tau_{av} = \Sigma A_i\tau_i/A_i = (I_1\tau_1 + I_2\tau_2) / (I_1 + I_2) \quad (6)$$

The energy transfer from WO_4^{2-} groups to the doping Eu^{3+} in $CdWO_4$:Eu^{3+} nanorods can be used to change the relative intensity of blue-green emission (WO_4^{2-}) and red emission (Eu^{3+}), and hence multi-color luminescence is realized. The effect of Eu^{3+} doping concentrations on the relative intensity of blue-green (WO_4^{2-}) and red emissions (Eu^{3+}) in $CdWO_4$:Eu^{3+} samples is shown in Fig. 4e. With increasing Eu^{3+} doping concentrations from 0.4% to 6.5%, the emission intensity of Eu^{3+} at 615 nm increases gradually until a maximum emission is reached at 4.0%, and then decreases at 6.5%. The decrease in emission intensity of Eu^{3+} is mainly due to the known concentration quenching effect at higher Eu^{3+} doping concentration. Correspondingly, the emission intensity of WO_4^{2-} groups at 475 nm decreases gradually, reaches a minimum value at 4.0%, and then increases at 6.5%, as shown in Fig. 4f. The contrary changes in the relative intensity between blue-green and red emissions as a function of Eu^{3+} concentration increase also suggests the existence of energy transfer from WO_4^{2-} groups to the doping Eu^{3+}. It should be denoted that the multi-color luminescence properties for $CdWO_4$:Eu^{3+} nanorods could be further improved via optimizing the Eu^{3+} doping concentration.

In order to further prove the energy transfer between WO_4^{2-} groups and Eu^{3+}, the luminescence decay curves for $^5D_0 \rightarrow {}^7F_2$ emission (615 nm) of $CdWO_4$:x%Eu^{3+} samples excited at 290 and 394 nm were measured, respectively. As mentioned above, when the WO_4^{2-} groups was excited with 290 nm UV light, all luminescence decay curves of $CdWO_4$:x%Eu^{3+} samples can be fitted into a double exponential behavior (For comparation, the luminescence decay curves and the fitted results of $CdWO_4$:0.4%Eu^{3+} and $CdWO_4$:4.0%Eu^{3+} were also given in Fig. S3 (a) and (c), ESI†). The values of the average lifetime determined by Eq. (6) were listed in Table S1 (ESI†). However, when the doping Eu^{3+} ions were excited with 394 nm UV light, all luminescence decay curves of these samples can be fitted into a single exponential function as Eq. (2), and the decay curves, the fitted results and the lifetimes were given in Fig. S3 (b, d) and Table S1 (ESI†), respectively. The decay behaviors at different excitation wavelenght also indicate the existence of energy transfer between WO_4^{2-} groups and Eu^{3+} in $CdWO_4$:Eu^{3+} samples. It is observed from Table S1 (ESI†) that the lifetime values increase when changing Eu^{3+} doping concentrations up to 4.0%, similar to the observation on the emission spectra of the samples under 290 nm excitation.[39] Moreover, the lifetime values measured under 394 nm excitation is shorter than those under 290 nm excitation. The obtained results here are consistent with the previous reports.[40]

The luminescence decay curves of host materials in the Eu^{3+} doped samples (λ_{ex} = 290 nm, λ_{em} = 475 nm) can also be well fitted into a single exponential function (Fig. S3 e and f) (ESI†), similar to that of the undoped $CdWO_4$ nanorods. However, it is noticeable that the lifetime values of $CdWO_4$:x%Eu^{3+} (x = 0.4, 1.2, 2.0, 4.0 and 6.5) are shorter compared to undoped $CdWO_4$ nanorods in Table 2. It is apparent that the energy transfer is occurred from WO_4^{2-} groups to Eu^{3+}. Using these lifetime values, a simple operational definition of energy transfer efficiency (η_{ET}) and energy transfer rate (ω_{ET}) of WO_4^{2-}- Eu^{3+} can be determined by [41]

$$\eta_{ET} = 1 - \frac{\tau_s}{\tau_{s0}} \quad (7)$$

$$\omega_{ET} = \frac{1}{\tau_s} - \frac{1}{\tau_{s0}} \quad (8)$$

where τ_s and τ_{s0} are the lifetimes of WO_4^{2-} with doped and undoped Eu^{3+} respectively. The values of η_{ET} and ω_{ET} are summarized in Table 2.

Table 2 Luminescence lifetime (τ), energy transfer efficiency (η_{ET}) and energy transfer rate (ω_{ET}) of $CdWO_4$:x%Eu^{3+} (x = 0, 0.4, 1.2, 2.0, 4.0 and 6.5) with λ_{ex} = 290 nm and λ_{em} = 475 nm.

Sample	τ/μs	η_{ET}	ω_{ET}/s^{-1}
$CdWO_4$	57.78		
$CdWO_4$:0.4%Eu^{3+}	15.16	73.8%	4.86×10^4
$CdWO_4$:1.2%Eu^{3+}	15.01	74.0%	4.93×10^4
$CdWO_4$:2.0%Eu^{3+}	15.92	72.4%	4.55×10^4
$CdWO_4$:4.0%Eu^{3+}	15.16	73.8%	4.86×10^4
$CdWO_4$:6.5%Eu^{3+}	11.72	79.7%	6.81×10^4

The energy transfer process in $CdWO_4$:Eu^{3+} is shown in Fig. 5. When excited by UV at 290 nm, electrons in the ground state ($^1A_1$) are excited into the ^1B ($^1T_2$) level of WO_4^{2-}. The electrons in excited state can either relax to the lowest excited ^1B ($^1T_2$) level of WO_4^{2-}, producing the emission through the transition to the $^1A_1$ level, or transfer the excited energy to the level of $^5D_3$ or higher levels in Eu^{3+} through a resonance process.[19] The energy nonradiatively relaxes from these high energy levels to the $^5D_0$ level by multiphonon relaxation. Then the characteristic emissions of Eu^{3+} due to $^5D_0 \rightarrow {}^7F_J$ (J = 1, 2, 3, 4) transitions are occured.[42-44]

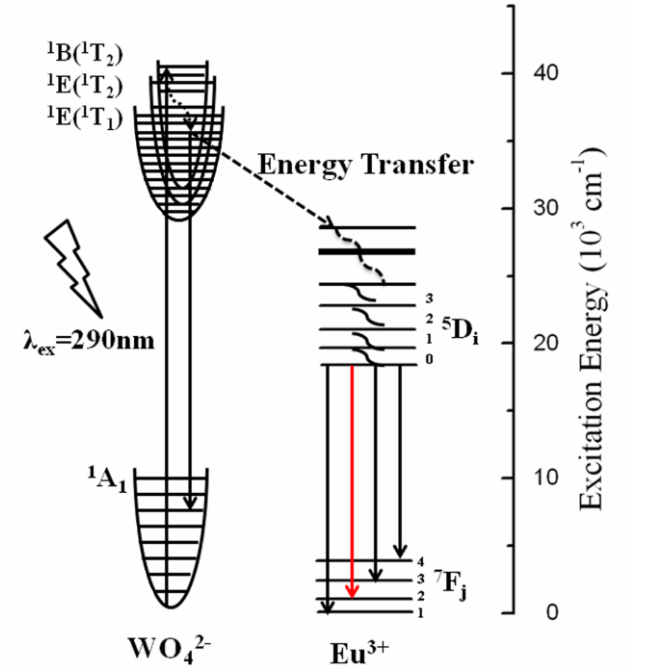

Fig. 5 Energy level scheme for WO_4^{2-} group and the energy transfer process from WO_4^{2-} to Eu^{3+} as well as the emission process from Eu^{3+}.

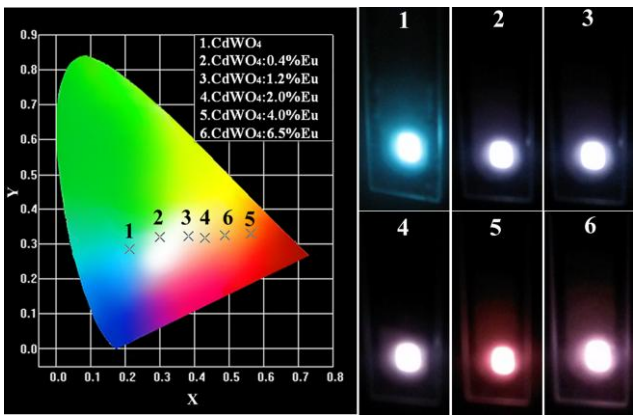

Fig. 6 CIE chromaticity diagram and luminescence photographs of $CdWO_4$:Eu^{3+} with different doping concentrations (0%, 0.4%, 1.2%, 2.0%, 4.0%, 6.5%).

The CIE diagram of the $CdWO_4$ with different Eu^{3+} doping concentrations is shown in Fig 6 (left). It can be seen that $CdWO_4$:x%Eu^{3+}(x = 0, 0.4, 1.2, 2.0, 4.0, 6.5) can emit blue-green, white, white, light red, bright red and dark red, respectively. $CdWO_4$:4.0%Eu^{3+} nanorods show bright and high color saturation because the $^5D_0$-$^7F_2$ transition of Eu^{3+} increases to the maximum at the doping concentration of 4.0%. The PL quantum efficiency of the $CdWO_4$ host, $CdWO_4$:0.4%Eu^{3+} and $CdWO_4$:4.0%Eu^{3+} nanorods are 30.35%, 2.07% and 9.75%, respectively. Fig. 6 (right) gives the emitting photographs of $CdWO_4$:x%Eu^{3+} samples under the irradiation of 290 nm UV light, corresponding to the sample points as shown in CIE chromaticity diagram.

Conclusion

In summary, uniform undoped or Eu^{3+} doped $CdWO_4$ nanorods have been prepared by a simple hydrothermal method and further characterized by various techniques of structure and luminescence. The $CdWO_4$ based samples have monoclinic phase structure at the doping concentrations of 0.4%~4.0%, and the nanorod-like morphology can be maintained when the doping concentration is lower than 6.5%. Due to the combination of the relative intensities from blue-green emission in intrinsic WO_4^{2-} complex and red emission in doping Eu^{3+} ions, the multi-color luminescence can be realized in the same $CdWO_4$ host under single excited wavelength simply via altering Eu^{3+} doping concentration. These luminescent nanomaterials may have a potential for the applications in displays, light sources, bio-imaging and so on.

Acknowledgements

This work is financially supported by the National Natural Science Foundation of China (no. 21171179, 21401218, 51272218), Excellent Youth Foundation of He'nan Scientific Committee (no. 134100510018), Innovation Scientists and Technicians Troop Construction Projects of Henan Province (no. 2013259), and Program for Innovative Research Team (in Science and Technology) in University of Henan Province (no. 14IRTSTHN009).

Notes and references

[a]*The Key Laboratory of Rare Earth Functional Materials and Applications, Zhoukou Normal University, Zhoukou 466001, P. R. China. E-mail: zlwang2007@hotmail.com; Fax: +86-394-8178518; Tel: +86-394-8178518*
[b]*The College of Chemistry and Molecular Engineering, Zhengzhou University, Zhengzhou 450001, P. R. China*
[c]*University Research Facility in Materials Characterization and Device F abrication, The Hong Kong Polytechnic University, Hong Kong, P. R. China.*
[d]*Department of Applied Physics, The Hong Kong Polytechnic University, Hong Kong; The Hong Kong Polytechnic University Shenzhen Research Institute, Shenzhen 518057, P. R. China.*
E-mail: jh.hao@polyu.edu.hk

†Electronic Supplementary Information (ESI) available: [TEM images of $CdWO_4$, $CdWO_4$:2.0%Eu^{3+}, $CdWO_4$:4.0%Eu^{3+} and $CdWO_4$:6.5%Eu^{3+} samples, luminescence decay curves and lifetimes]. See DOI: 10.1039/b000000x/

1 (a) J. Feng and H. J. Zhang, *Chem. Soc. Rev.*, 2013, **42**, 387; (b) A. J. Rondinone, M. Pawel, D. Travaglini, S. Mahurin and S. Dai, *J. Colloid. Interf. Sci.*, 2007, **306**, 281; (c) H. W. Liao, Y. F. Wang, X. M. Liu, Y. D. Li and Y. T. Qian, *Chem. Mater.*, 2000, **12**, 2819.
2 (a) W. D. Shi, S. Y. Song and H. J. Zhang *Chem. Soc. Rev.*, 2013, **42**, 5714; (b) H. L. Wang, X. D. Ma, X. F. Qian, J. Yin and Z. K. Zhu, *J. Solid State Chem.*, 2004, **177**, 4588; (c) R. P. Jia, G. X. Zhang, Q. S. Wu and Y. P. Ding, *Appl. Sur. Sci.*, 2006, **253**, 2038.
3 (a) W. Tong, L. Li, W. Hu, T. Yan and G. Li, *J. Phys. Chem. C*, 2010, **114**, 1512; (b) C. S. Lim, *Mater. Chem. Phys.*, 2012, **131**, 714; (c) V. V. Laguta, M. Nikl, J. Rosa, B. V. Grinyov, L. L. Nagornaya and I. A. Tupitsina, *J. Appl. Phys.*, 2008, **104**, 103525.
4 (a) T. Yan, L. Li, W. Tong, J. Zheng, Y. Wang and G. Li, *J. Solid State Chem.*, 2011, **184**, 357; (b) Z. L. Wang, H. L. Li, and J. H. Hao, *J. Electrochem. Soc.*, 2008, **155**, J152; (c) H. L. Li, Z. L. Wang, S. J. Xu and J. H. Hao, *J. Electrochem. Soc.*, 2009, **156**, J112; (d) Y. Zhang and J. H. Hao, *J. Mater. Chem. C*, 2013, **1**, 5607.
5 Y. Ling, L. Zhou, L. Tan, Y. Wang and C. Yu, *CrystEngComm*, 2010, **12**, 3019.
6 S. H. Yu, M. Antonietti, H. Cölfen and M. Giersig, *Angew. Chem.*, 2002, **114**, 2462.

7 G. X. Zhang, S. F. Yang, Z. Li, L. Zhang, W. Zhou, H. Y. Zhang, H. Shen and Y. X. Wang, *Appl. Surf. Sci.*, 2010, **257**, 302.
8 Z. J. Wang, J. P. Zhong, H. X. Jiang, J. Wang and H. B. Liang, *Cryst. Growth Des.*, 2014, **14**, 3767.
9 D. Li, X. Bai, J. Xu, X. Ma and Y. Zhu, *Phys. Chem. Chem. Phys.*, 2014, **16**, 212.
10 D. Ye, D. Z. Li, W. J. Zhang, M. Sun, Y. Hu, Y. F. Zhang and X. Z. Fu, *J. Phys. Chem. C*, 2008, **112**, 17351.
11 L. Wang and W. Z. Wang, *CrystEngComm*, 2012, **14**, 3315.
12 S. Wang, J. Feng, S. Song and H. Zhang, *CrystEngComm*, 2013, **15**, 7142.
13 Y. J. Wang, X. F. Guan, L. P. Li, H. Lin, X. X. Wang and G. S. Li, *New J. Chem.*, 2012, **36**, 1852.
14 J. Xu, M. Chen and Z. Wang, *Dalton Trans.*, 2014, **43**, 3537.
15 D. Ye, D. Z. Li, W. Chen, Y. Shao, G. C. Xiao, M. Sun and X. Z. Fu, *Res. Chem. Intermed.*, 2009, **35**, 675.
16 M. J. You, J. Y. Xu, Z. J. Zhang and Y. Zhou, *Ceram. Int.*, 2014, **40**,16189.
17 Q. L. Dai, H. W. Song, G. H. Pan, X. Bai, H. Zhang, R. F. Qin, L. Y. Hu, H. F. Zhao, S. Z. Lu and X. G. Ren, *J. Appl. Phys.*, 2007, **102**, 054311.
18 Z. L. Wang, G. Z. Li, Z. W. Quan, D. Y. Kong, X. M. Liu, M. Yu and J. Lin, *J. Nanosci. Nanotechnol.*, 2007, **7**, 602.
19 W. Wang, P. Yang, Z. Cheng, Z. Hou, C. Li and J. Lin, *ACS Appl. Mater. Interf.*, 2011, **3**, 3921.
20 Y. Su, L. Li and G. Li, *Chem. Mater.*, 2008, **20**, 6060.
21 R. D. Shannon, *Acta Cryst. Sect. A*, 1976, **32**, 751.
22 R. Okram, N. Yaiphaba, R. S. Ningthoujam and N. R. Singh, *Inorg. Chem.*, 2014, **53**, 7204.
23 (a) J. Wang, S. B. Wang and Q. Su, *J. Mater. Chem.*, 2004, **14**, 2569; (b) Y. L. Liu, J. Y. Kuang, B. F. Lei and C. S. Shi, *J. Mater. Chem.*, 2005, **15**, 4025.
24 F. Wang, Y. Han, C. S. Lim, Y. H. Lu, J. Wang, J. Xu, H. Y. Chen, C. Zhang, M. H. Hong and X. G. Liu, *Nature*, 2010, **463**, 1061.
25 L.Y. Wang and Y. D. Li, *Chem. Mater.*, 2007, **19**, 727.
26 D. Yue, C. Y. Li, W. Lu, X. L. Zhang, J. Z. Chang and Z. L. Wang, *Acta Chim. Sinica*, 2012, **70**, 1812 (in Chinese).
27 Y. L. Huang and H. J. Seo, *J. Phys. Chem. A*, 2009, **113**, 5317.
28 C. Y. Li, X. D. Du, D. Yue, J. N. Gao and Z. L. Wang, *Mater. Lett.*, 2013, **108**, 257.
29 M. Mai and C. Feldmann, *J. Mater. Sci.*, 2012, **47**, 1427.
30 Y. Su, L. Li and G. Li, *J. Mater. Chem.*, 2009, **19**, 2316.
31 Z. L. Wang, M. Li, C. Wang, J. Z. Chang, H. Z. Shi and J. Lin, *J. Rare Earth*, 2009, **27**, 33.
32 Z. L. Wang, J. H. Hao and H. L. Chan, *CrystEngComm*, 2010, **12**, 1373.
33 S. Y. Song, Y. Zhang, J. Feng, X. Ge, D. P. Liu, W. Q. Fan, Y. Q. Lei, Y. Xing and H. J. Zhang, *CrystEngComm*, 2009, **11**, 1987.
34 F. W. Kang, Y. H. Hu, L. Chen, X. J. Wang, H. Y. Wu and Z. F. Mu, *J. Lumin.*, 2013, **135**, 113.
35 (a) A. K. Parchur, A. I. Prasad, A. A. Ansari, S. B. Raia and R. S. Ningthoujam, *Dalton Trans.*, 2012, **41**, 11032; (b) N. K. Sahu, N. S. Singh, R. S. Ningthoujam and D. Bahadur, *ACS Photonics*, 2014, **1**, 337
36 (a) A.M. Kaczmarek and R. V. Deun, *Chem. Soc. Rev.*, 2013, **42**, 8835; (b) F. Wang, R. R. Deng, J. Wang, Q. X. Wang, Y. Han, H. M. Zhu, X. Y. Chen and X. G. Liu, *Nature Mater.*, 2011, **10**, 968; (c) L. L. Wang, Q. L. Wang, X. Y. Xu, J. Z. Li, L. B. Gao, W. K. Kang, J. S Shi and J. Wang, *J. Mater. Chem. C*, 2013, **1**, 8033.
37 A. K. Parchur and R. S. Ningthoujam, *RSC Adv.*, 2012, **2**, 10859.
38 D. P. Dutta, R. S. Ningthoujam and A. K. Tyagi, *AIP Adv.*, 2012, **2**, 042184.
39 N. S. Singh, R. S. Ningthoujam, G. Phaomei, S. D. Singh, A. Vinud and R. K. Vatsab *Dalton Trans.*, 2012, **41**, 4404.
40 A. K. Parchur, R. S. Ningthoujam, S. B. Rai, G. S. Okram, R. A. Singh, M. Tyagi, S. C. Gadkari, R. Tewari and R. K. Vatsa, *Dalton Trans.*, 2011, **40**, 7595.
41 (a) P. I. Paulose, G. Jose, V. Thomas, N. V. Unnikrishnan and M. Warrier, *J. Phys. Chem. Solids*, 2003, **64**, 841; (b) G. A. Hebbink, L. Grave, L. A. Woldering, D. N. Reinhoudt and F. Veggel, *J. Phys. Chem. A*, 2003, **107**, 2483; (c) S. Balaji, A. K. Mandal and K. Annapurna, *Opt. Mater.*, 2012, **34**, 1930; (d) P. Vergeer, T. J. H. Vlugt, M. H. F. Kox, M. I. den Hertog, J. P. J. M. van der Eerden and A. Meijerink, *Phys. Rev. B*, 2005, **71**, 014119; (e) A. K. Parchur, A. I. Prasad, S. B. Rai and R. S. Ningthoujam, *Dalton Trans.*, 2012, **41**, 13810.
42 G. Blasse and B. C. Grabmaier, in *Luminescent Materials*, Springer-Verlag, Berlin Heidelberg, 1994, Ch. 4.
43 P. Y. Jia, X. M. Liu, G. Li, M. Yu, J. Fang and J. Lin, *Nanotechnology*, 2006, **17**, 734.
44 M. J. Treadaway and R. C. Powell, *J. Chem. Phys.*, 1974, **61**, 4003.

Multi-color Luminescence of Uniform $CdWO_4$ Nanorods through Eu^{3+} Ion Doping

Dan Yue,[a,b] Qingfeng Li,[a] Wei Lu,[c] Qi Wang,[a] Mengnan Wang,[a,b] Chunyang Li,[a] Lin Jin ,[a] Yurong Shi,[a] Zhenling Wang,[*,a] Jianhua Hao[*,d]

Multi-color luminescence of uniform $CdWO_4$: Eu^{3+} nanorods can be realized only through altering the doping concentration of Eu^{3+} ions.

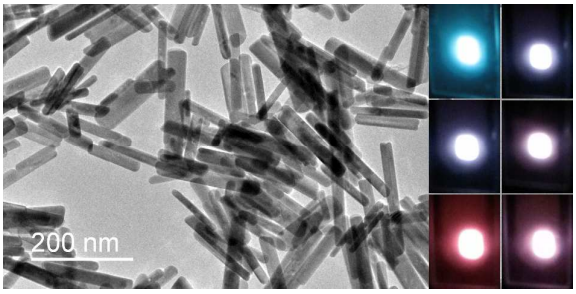

TOC Figure